ADER High-Order Schemes for Evolutionary PDEs: a Brief Review

E. F. Toro, C. E. Castro and M. Dumbser
Laboratory of Applied Mathematics
Department of Civil and Environmental Engineering
University of Trento, Italy

Abstract. We give an overview of the ADER approach for constructing numerical schemes of arbitrary order of accuracy in space and time, for solving evolutionary partial differential equations.

1 Introduction

Most of the current experience with ADER methods relate to non-linear hyperbolic systems of balance laws

$$\partial_t \mathbf{Q} + \partial_x \mathbf{F}(\mathbf{Q}) + \partial_y \mathbf{G}(\mathbf{Q}) + \partial_z \mathbf{H}(\mathbf{Q}) = \mathbf{S}(\mathbf{Q}) \ , \tag{1}$$

where $\mathbf{Q}$ is the vector of unknowns, $\mathbf{F}(\mathbf{Q})$, $\mathbf{G}(\mathbf{Q})$, $\mathbf{H}(\mathbf{Q})$ are prescribed flux functions and $\mathbf{S}(\mathbf{Q})$ is the vector of source terms (stiff or non-stiff). Recent work extends the ADER methodology to solve non-linear reaction-diffusion equations, which in one space dimension read

$$\partial_t \mathbf{Q}(x,t) = \partial_x \left(\alpha(x,t,\mathbf{Q}(x,t)) \partial_x \mathbf{Q}(x,t) \right) + \mathbf{S}(\mathbf{Q}(x,t)) \ , \tag{2}$$

where $\mathbf{Q}(x,t)$ is the unknown of the problem, $\alpha(x,t,\mathbf{Q}(x,t))$ is a prescribed diffusion coefficient and $\mathbf{S}(x,t,\mathbf{Q}(x,t))$ is a reaction (source) term.

The ADER approach can be implemented in two major existing frameworks: finite volumes and discontinuous Galerkin finite elements. In the finite volume framework the ADER approach contains three main steps, namely (i) a non-oscillatory spatial reconstruction using cell averages, (ii) solution of high-order Riemann problems at the interface to define the numerical flux, and in the presence of source terms, (iii) evaluation of a volume integral to high accuracy in space and time to define the numerical source.

The reconstruction problem can be viewed in different ways. The simplest is that in which solutions do no include large spatial gradients or discontinuities and one can use *fixed-stencil*, or linear, reconstructions. For problems involving large gradients and shocks one must use non-linear, or solution adaptive, reconstructions. Here one must make the distinction between structured and unstructured meshes.

Preliminary results on the ADER approach are found in [29] for linear problems on structured meshes. Further developments of the approach are reported in [30], [26], [25],[21], [15], [22], [16] [20], [31], [27], [5], [4], [6], [17], [5], [4], [6], [7], [8], [2], [36], [33], [9] .

Sect. 2 discuses the high-order Riemann problem, Sect. 3 shows some examples and Sect. 3 draws some conclusions.

2 The High-Order Riemann Problem

We assume that an appropriate spatial reconstruction method from cell averages is in place. For this we recommend the recently proposed WENO procedure [6], [7]. Then, at each interface, there will be a discontinuity surface. To determine the numerical flux we require the solution, as a function of time, at each integration point. For this we need to solve a high-order Riemann problem. Here we first state the mathematical problem and then briefly review existing methods to compute the solution at the interface, as a function of time.

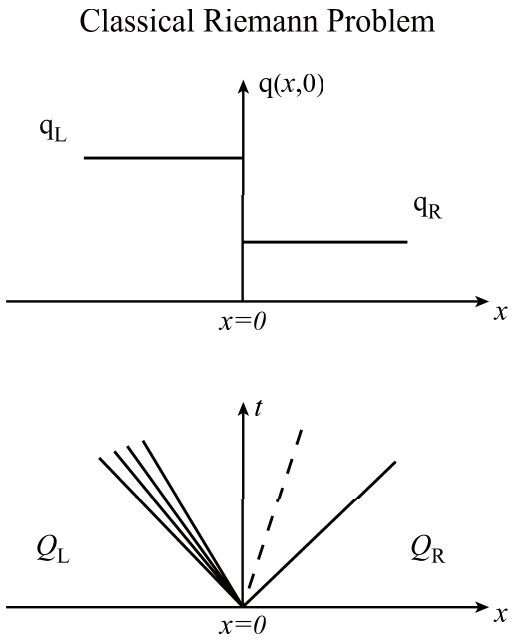

Figure 1: The classical Riemann problem for a typical 3×3 non-linear homogeneous system. Top frame: initial condition at $t = 0$ for a single component q of the vector of unknowns $\mathbf{Q}$. Bottom frame: structure of the similarity solution in the $x - t$ plane.

2.1 The mathematical problem

The high-order Riemann problem (often called the Generalized Riemann Problem, or the Derivative Riemann Problem) is the initial-value problem

$$\left.\begin{array}{ll} \text{PDEs:} & \partial_t \mathbf{Q} + \partial_x \mathbf{F}(\mathbf{Q}) = \mathbf{S}(\mathbf{Q}) \ , \quad x \in (-\infty, \infty) \ , \quad t > 0 \ , \\ \text{IC:} & \mathbf{Q}(x,0) = \left\{ \begin{array}{ll} \mathbf{Q}_L(x) & \text{if} \quad x < 0 \ , \\ \mathbf{Q}_R(x) & \text{if} \quad x > 0 \ . \end{array} \right. \end{array} \right\} \tag{3}$$

The partial differential equations (PDEs), with source terms, are assumed to be a general system of hyperbolic balance laws. The initial condition (IC) consists of two vectors $\mathbf{Q}_L(x)$ and $\mathbf{Q}_R(x)$, the components of which are assumed to be smooth functions of x, with K continuous non-trivial spatial derivatives away from zero. We denote by DRP_K the case in which the initial conditions in (3) consist of polynomials of degree at most K. The case DRP_0 corresponds to the *classical* piece-wise constant data Riemann problem, associated with the first-order Godunov scheme [10]. Similarly, case DRP_1 corresponds to the piece-wise linear data Riemann problem, or the so-called generalized Riemann problem (GRP), associated with a second-order method of the Godunov type [18], [34], [1], [3], [28].

Fig. 1 depicts the classical Riemann problem DRP_0 for a typical 3×3 homogeneous non-linear system. The bottom frame of Fig. 1 depicts the structure of the corresponding solution in the $x-t$ plane; characteristic curves are straight lines. We note however, that the solution of the Riemann problem with piece-wise constant data but with source terms does not have a similarity solution and cannot be represented as in Fig. 1 (bottom frame).

Fig. 2 illustrates the high-order Riemann problem DRP_K; the top frame depicts the initial condition for a single component q; data consists of two smooth vectors separated by a discontinuity at the origin. The bottom frame of Fig. 2 depicts the corresponding structure of the solution in the $x - t$ plane. Now characteristics are no longer straight lines. Compare Figs. 1 and 2.

For numerical purposes it is sufficient to find the solution of (3) at the origin $x = 0$ and for $t > 0$,

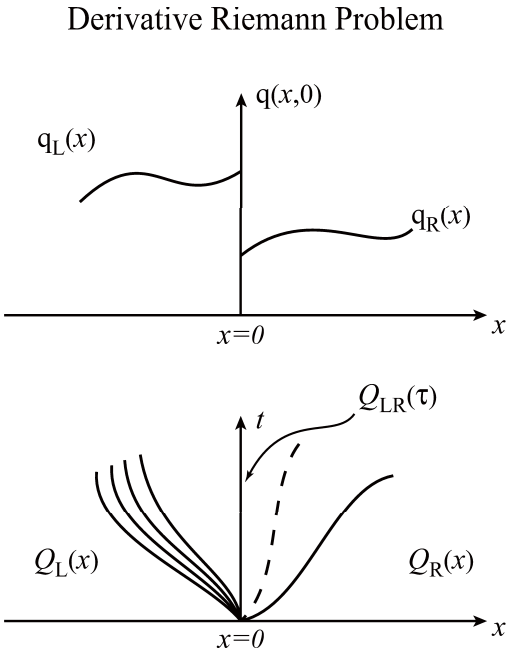

Figure 2: The Derivative Riemann Problem for a typical 3×3 non-linear system. Top frame: initial condition at $t=0$ for a single component q of the vector of unknowns $\mathbf{Q}$. Bottom frame: structure of the solution on the $x-t$ plane.

as a function of time, denoted by $Q_{LR}(\tau)$ in Fig. 2.

To construct high-order numerical methods of the ADER type of $(K+1)$-th order of accuracy in both space and time it is sufficient to find the solution $Q_{LR}(\tau)$ of (3). The corresponding intercell numerical flux results from evaluating the integral

$$\mathbf{F}_{LR}=\frac{1}{\Delta t}\int_0^{\Delta t}\mathbf{F}(\mathbf{Q}_{LR}(\tau))d\tau\ , \tag{4}$$

where Δt is the time step of the scheme.

2.2 Solvers for the High-Order Riemann Problem

Here we very briefly review four existing solvers for the high-order Riemann problem.

2.2.1 The Toro-Titarev solver

The method proposed by Toro and Titarev [30], [32] first expresses the solution $\mathbf{Q}_{LR}(\tau)$ at the interface $x=0$ as the power series expansion in time

$$\mathbf{Q}_{LR}(\tau)=\mathbf{Q}(0,0_+)+\sum_{k=1}^{K}\left[\partial_t^{(k)}\mathbf{Q}(0,0_+)\right]\frac{\tau^k}{k!}\ . \tag{5}$$

The leading term $\mathbf{Q}(0,0_+)$ is found by solving a conventional (non-linear) Riemann problem using as data the extrapolated values from left and right in (1). The higher-order terms require the determination of the coefficients $\partial_t^{(k)}\mathbf{Q}(0,0_+)$. This part includes the following steps: (a) use the Cauchy-Kowalewski procedure to express all time derivatives $\partial_t^{(k)}\mathbf{Q}(0,0_+)$ as functions $\mathbf{G}^{(k)}$ of spatial derivatives, namely

$$\partial_t^{(k)}\mathbf{Q}(x,t)=\mathbf{G}^{(k)}\left(\partial_x^{(0)}\mathbf{Q},\partial_x^{(1)}\mathbf{Q},\ldots,\partial_x^{(k)}\mathbf{Q}\right)\ , \tag{6}$$

(b) solve classical linear Riemann problems for the spatial derivatives $\partial_x^{(l)}\mathbf{Q}$ to determined the arguments of $\mathbf{G}^{(k)}$, which then give the coefficients $\partial_t^{(k)}\mathbf{Q}(0,0_+)$. This solution technique for DRP_K reduces the problem to that of solving $K+1$ classical homogeneous Riemann problems, one (generally non-linear) Riemann problem to compute the leading term, and K linearized Riemann problems to determine the higher order terms. See [7] for details on a subroutine for performing the Cauchy-Kowalewski procedure for the three-dimensional Euler equations.

2.2.2 The Harten-Engquist-Osher-Chakravarthy (HEOC) solver

The Harten-Engquist-Osher-Chakravarthy (HEOC) solver results from a re-interpretation of the high-order method of [11], see [2] for details. This method first evolves in time the initial conditions by developing power series expansions in time on each side of the interface, namely

$$\left.\begin{array}{l} \tilde{\mathbf{Q}}_L(\tau) = \mathbf{Q}_L(0_-) + \sum_{k=1}^{K} \left[\partial_t^{(k)}\mathbf{Q}(0_-,0)\right] \frac{\tau^k}{k!} \\ \tilde{\mathbf{Q}}_R(\tau) = \mathbf{Q}_R(0_+) + \sum_{k=1}^{K} \left[\partial_t^{(k)}\mathbf{Q}(0_+,0)\right] \frac{\tau^k}{k!} \end{array}\right\} . \tag{7}$$

The Cauchy-Kowalewski procedure then allows the use of the PDEs in (3) to express all time derivatives in (7) as functions of space derivatives and of the source terms, as in (6). The spatial derivatives are calculated as the limiting values from left and right, at $t=0$, of the spatial derivatives of the initial conditions, denoted as $\mathbf{Q}_L^{(k)}(0_-)$, $\mathbf{Q}_R^{(k)}(0_-)$. Then

$$\left.\begin{array}{l} \partial_t^{(k)}\mathbf{Q}(0_-,0) = \mathbf{G}^{(k)}\left(\mathbf{Q}_L^{(0)}(0_-), \mathbf{Q}_L^{(1)}(0_-), \ldots, \mathbf{Q}_L^{(k)}(0_-)\right) \\ \partial_t^{(k)}\mathbf{Q}(0_+,0) = \mathbf{G}^{(k)}\left(\mathbf{Q}_R^{(0)}(0_+), \mathbf{Q}_L^{(1)}(0_+), \ldots, \mathbf{Q}_L^{(k)}(0_+)\right) \end{array}\right\} \tag{8}$$

are determined and thus the expansions (7) are determined at any time $t=\tau$.

Finally one defines the solution of the DRP (3) at the interface $x=0$, at time $t=\tau$ as $\mathbf{Q}_{LR}(\tau) = \mathbf{D}(\tau,0)$, where now $\mathbf{D}(\tau, x/(t-\tau))$ is the similarity solution of the classical, homogeneous Riemann problem

$$\left.\begin{array}{ll} \text{PDEs:} & \partial_t\mathbf{Q} + \partial_x\mathbf{F}(\mathbf{Q}) = \mathbf{0}\ , \\ \text{ICs:} & \mathbf{Q}(x,0) = \left\{\begin{array}{lll} \tilde{\mathbf{Q}}_L(\tau) & \text{if} & x<0\ , \\ \tilde{\mathbf{Q}}_R(\tau) & \text{if} & x>0\ . \end{array}\right. \end{array}\right\} \tag{9}$$

Note that here $\mathbf{D}(\tau, x/(t-\tau))$ depends on the parameter τ.

Fig. 3 gives an interpretation of the HEOC solution method for the DRP (3). At time $t=0$ one performs a series expansion in time on the limiting values of the data left and right of the interface (circles). Via the Cauchy-Kowalewski method one evolves the data in time on each side of the interface, to produce time-evolved states $\tilde{\mathbf{Q}}_L(\tau)$ and $\tilde{\mathbf{Q}}_R(\tau)$, at any chosen time $t=\tau$ (rhombuses in Fig. 3). These (constant) states at $t=\tau$ form the initial conditions for a classical Riemann problem, as depicted on the top part of Fig. 3 by the self-similar wave pattern. The sought solution is that given by (9), which is constant along the t-axis associated with the self-similar wave pattern. As the method applies to any time τ one has a time-dependent solution $\mathbf{Q}_{LR}(\tau)$ at the interface.

We remark that, just as in the Toro-Titarev solver [30], the HEOC solution method applies to in-homogeneous non-linear conservation balance laws. The influence of the source term enters via the Cauchy-Kowalewski method, in which the source terms enter the coefficients in (7), (8). But note that at no point in the method it becomes necessary to solve Riemann problems, explicitly accounting for the influence of the source terms.

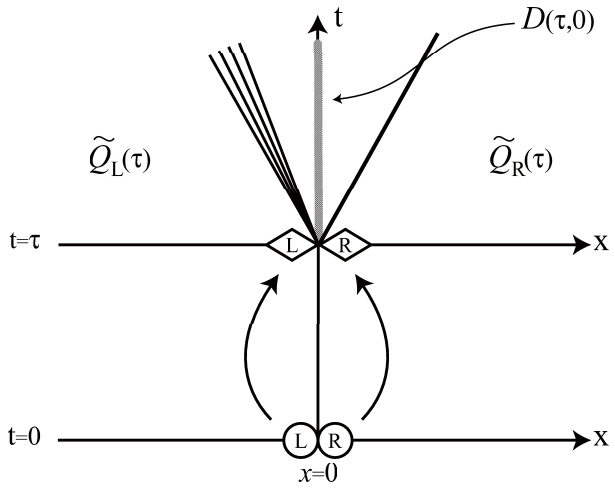

Figure 3: Illustration of the HEOC Derivative Riemann Problem solver. The limiting values of the initial data from left and right (circles) are time evolved separately to any time τ (rhombuses). The desired solution results from solving the classical Riemann problem with these evolved states as data.

2.2.3 The Castro-Toro solver

The sought solution at the interface is again expressed as in (5), with the leading term computed as in the Toro-Titarev solver. To compute the higher order terms we solve *time-derivative* Riemann problems, that is, for any index $k > 0$ we compute $\partial_t^{(k)}\mathbf{Q}(0_-, 0)$ and $\partial_t^{(k)}\mathbf{Q}(0_+, 0)$ as in (8). To find $\partial_t^{(k)}\mathbf{Q}(0, 0_+)$ right at the interface one solves the classical linearized homogeneous Riemann problem

$$\left.\begin{array}{ll} \text{PDEs:} & \partial_t\Big(\partial_t^{(k)}\mathbf{Q}(x,t)\Big) + \mathbf{A}_{LR}^{(0)}\,\partial_x\Big(\partial_t^{(k)}\mathbf{Q}(x,t)\Big) = \mathbf{0}\,, \\ \text{ICs:} & \partial_t^{(k)}\mathbf{Q}(x,0) = \left\{\begin{array}{ll} \partial_t^{(k)}\mathbf{Q}(0_-,0) & \text{if} \quad x < 0\,, \\ \partial_t^{(k)}\mathbf{Q}(0_+,0) & \text{if} \quad x > 0\,. \end{array}\right. \end{array}\right\} \tag{10}$$

The similarity solution is denoted by $\mathbf{T}^{(k)}(x/t)$ and the sought value is

$$\partial_t^{(k)}\mathbf{Q}(0, 0_+) = \mathbf{T}^{(k)}(0)\,. \tag{11}$$

2.2.4 The Dumbser-Enaux-Toro (DET) solver

An alternative solver for the high-order Riemann problem has recently been proposed by Dumbser et al. [8]. This is an entirely numerical solver. Here, instead of using the Cauchy-Kowaleski method to evolve the data (3), as done in the HEOC method, we evolve such data numerically. The basic concept of this approach is to construct a weak local formulation of the PDEs in space and time using a new local space-time discontinuous Galerkin approach. This results in small systems of nonlinear algebraic equations to solve, but no analytic differentiation of the governing equations is necessary. Then the interaction of the evolved data at the desired time $t = \tau$ requires the solution of the classical Riemann problem (3), as as for the HEOC solver. The advantages of this variant are twofold (i) one avoids the cumbersome Cauchy-Kowalewski procedure, resulting also in great generality; (ii) one can treat stiff source terms properly, reconciling the usually incompatible concepts of high accuracy and stiffness.

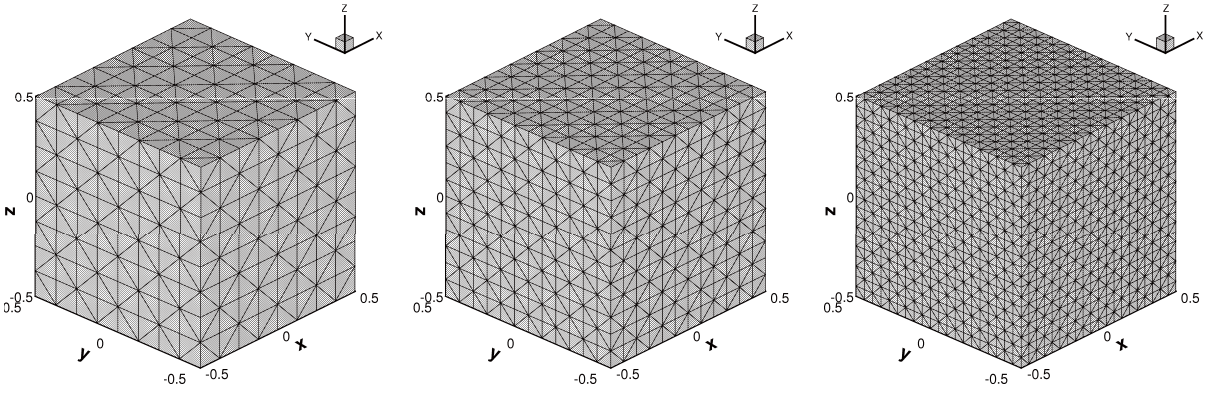

Figure 4: Sequence of regular tetrahedral meshes used for the three-dimensional convergence studies.

3 Sample Application

The purpose of this application is to address three main issues regarding high-order methods. The first is to do with accuracy; it is in our view mandatory to perform convergence rate studies to verify if the methods being developed or applied actually attain the claimed high order of accuracy in both space and time, and for realistic situations. The second issue refers to the ability of such high-order methods to perform satisfactorily for flows containing discontinuities, for which the concept of high accuracy does not apply. Thirdly, such methods must me applicable to solve problems in complex geometries, which usually must be discretized with unstructured meshes.

3.1 Convergence rate studies on unstructured meshes in 3D

In order to study the convergence behaviour of our method for the three dimensional compressible Euler equations we *create* a smooth unsteady test case with exact reference solution by prescribing a vector $U_p(\vec{x},t)$ which when substituted into the system of the Euler equations produces a modified Euler system with a source term. Note that for the test to be useful the method must be also capable of computing solutions to inhomogeneous problems, that is with a non-vanishing right-hand side, to the required order of accuracy. For details of the computational setup see [7]. Therefore, we now solve the three-dimensional Euler equations with source terms in the domain $\Omega_{3D} = [-0.5;0.5]^3$ with six periodic boundary conditions and the following exact solution to the problem that serves also as initial condition:

$$\begin{pmatrix} \rho \\ \vec{V} \\ p \end{pmatrix} (\vec{x},t) = \begin{pmatrix} 2 + A_0 \sin\left(\omega t - \vec{k}\vec{x}\right) \\ \vec{0} \\ 2 + A_0 \sin\left(\omega t - \vec{k}\vec{x}\right) \end{pmatrix}. \tag{12}$$

We note that the solution is simple but non-trivial. The constants are set to be $A_0 = 1.0$ and $\vec{k} = (k_x, k_y, k_z)$ with $k_x = k_y = k_z = \omega = 2\pi$. In this review paper we only present the convergence rates obtained with our ADER finite volume schemes on tetrahedral meshes for third and sixth order of accuracy, a more detailed study can be found in [7]. The errors presented in Table 1 are those for the velocity in x-direction, i.e. for the primitive variable u. Similar results are obtained for all the other flow quantities.

Table 1: Numerical convergence results obtained with ADER-FV schemes of third and sixth order in space and time for the three-dimensional test case after $t = 0.25$.

N_G	L^∞	L^1	L^2	$\mathcal{O}_{L^\infty}$	$\mathcal{O}_{L^1}$	$\mathcal{O}_{L^2}$	$t_{\mathrm{CPU}}[s]$
ADER-FV $\mathcal{O}3$ (M=2)							
8	2.3265E-02	8.7869E-03	1.0185E-02				4
12	8.0369E-03	2.4689E-03	2.9695E-03	2.6	3.1	3.0	17
16	3.5522E-03	1.0640E-03	1.2935E-03	2.8	2.9	2.9	54
20	1.7930E-03	5.4621E-04	6.6247E-04	3.1	3.0	3.0	130
24	9.9836E-04	3.1449E-04	3.8055E-04	3.2	3.0	3.0	260
32	4.1918E-04	1.3316E-04	1.6143E-04	3.0	3.0	3.0	820
4	3.1815E-02	1.1310E-02	1.3915E-02				1
8	1.3728E-03	1.4197E-04	1.7917E-04	4.5	6.3	6.3	20
12	2.1289E-04	1.0618E-05	1.6858E-05	4.6	6.4	5.8	143
16	3.1281E-05	1.6605E-06	2.3375E-06	6.7	6.4	6.9	467
20	7.4469E-06	4.1553E-07	6.1345E-07	6.4	6.2	6.0	1153
24	2.2733E-06	1.3416E-07	1.9236E-07	6.5	6.2	6.4	2304

3.2 Shock wave reflection problem

Here we illustrate the potential of the ADER methods to solve realistic problems to high accuracy on complicated domains using unstructured meshes. We consider the reflection of a plane shock wave from a solid body of triangular shape. The computational domain is $[-0.65, 0.5] \times [-0.5, 0.5]$, with a triangular solid body with vertexes $v_1 = (-0.2, 0)$, $v_2 = (0.1, -1/6)$ and $v_3 = (0.1, 1/6)$. The incident shock of shock Mach number $Ms = 1.3$ is placed at $x = -0.55$, at $t = 0$. Initial conditions ahead of the shock are $\rho = 1.225(kg/m^3)$, $p = 1.01325 \times 10^5(Pa)$ and zero velocity. Conditions behind the shock are obtained from the Rankine-Hugoniot conditions. The mesh consists of 256580 triangles and for the computations we use the Toro-Castro solver and a CFL coefficient $C_{cfl} = 0.45$.

A computational result at time $t = 2.20 \times 10^{-3}$ is shown in Fig. 5. The main physical features of the flow look reasonable, as compared with analogous problems for which there are experimental results, see [19], for example.

4 Concluding Remarks

A succinct review of the ADER approach has been presented, along with some illustrative examples and a list of relevant references.

In discussing high-order methods there is a crucial question to answer. Are these methods justified ? Or put in a different way, given an error, what is more convenient from the computational point of view, to solve the equations using a (simple) low-order method on a fine mesh, or use a (sophisticated) high-order method on a coarse mesh ? Our experience so far shows that the latter option is distinctively more convenient. That is, high-order methods are completely justified, specially if accurate (small errors) are required.

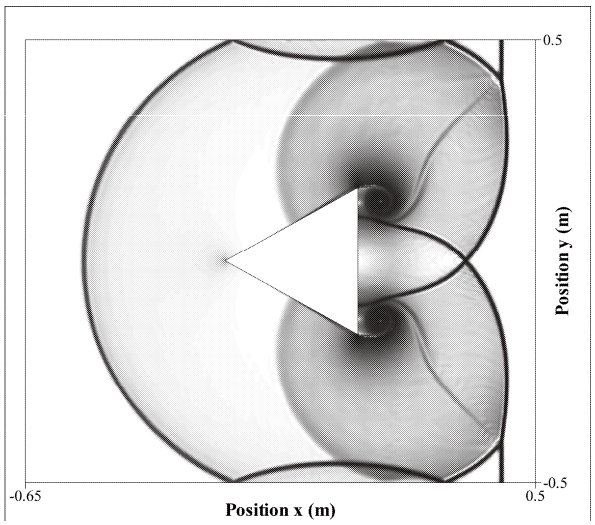

Figure 5: Shock wave reflection problem. Schlieren image for density at time $t = 2.20 \times 10^{-3}$. Two vortexes evolve behind the triangle. The expansion waves interact with the shock and with the boundaries.

References

[1] M. Ben-Artzi and J. Falcovitz. A Second Order Godunov–Type Scheme for Compressible Fluid Dynamics. *J. Comput. Phys.*, 55:1–32, 1984.

[2] C. E. Castro and E. F. Toro. Solvers for the High-Order Riemann Problem for Hyperbolic Balance Laws. *J. Comput. Phys.* (submitted), 2007.

[3] P. Colella. A Direct Eulerian MUSCL Scheme for Gas Dynamics. *SIAM J. Sci. Stat. Comput.*, 6:104–117, 1985.

[4] M. Dumbser. *Arbitrary High Order Schemes for the Solution of Hyperbolic Conservation Laws in Complex Domains.* PhD thesis, Institut für Aero- un Gasdynamik, Universität Stuttgart, Germany, 2005.

[5] M. Dumbser and C. D. Munz. ADER Discontinuous Galerkin Schemes for Aeroacoustics. *Comptes Rendus Mécanique*, 333:683–687, 2005.

[6] M. Dumbser and M. Käser. Arbitrary high order non-oscillatory finite volume schemes on unstructured meshes for linear hyperbolic systems. *J. Comp. Phys.*, 221:693–723, 2007.

[7] M. Dumbser, M. Käser, V. A. Titarev and E. F. Toro. Quadrature-free non-oscillatory finite volume schemes on unstructured meshes for nonlinear hyperbolic systems. *J. Comp. Phys.*, 226:204–243, 2007.

[8] M. Dumbser, C. Enaux, E. F. Toro. Explicit finite volume schemes of arbitrary high order of accuracy for hyperbolic systems with stiff source terms. *J. Comput. Phys.* (submitted), 2007.

[9] G. Gassner, F. Lorcher, C. D. MUnz. A contribution to the construction of diffusion fluxes for finite volume and discontinuous Galerkin schemes. *J. Comp. Phys.*, 224:1049-1063, 2007.

[10] S. K. Godunov. Finite Difference Methods for the Computation of Discontinuous Solutions of the Equations of Fluid Dynamics. *Mat. Sb.*, 47:271–306, 1959.

[11] A. Harten, B. Engquist, S. Osher, and S. R. Chakravarthy. Uniformly High Order Accuracy Essentially Non–oscillatory Schemes III. *J. Comput. Phys.*, 71:231–303, 1987.

[12] A. Harten and S. Osher. Uniformly High–Order Accurate Nonoscillatory Schemes I. *SIAM J. Numer. Anal.*, 24(2):279–309, 1987.

[13] C. Hu and C. W. Shu. Weighted Essentially Non-oscillatory Schemes on Triangular Meshes. *J. Comp. Phys.*, 150:97–127, 1999.

[14] G. S. Jiang and C. W. Shu. Efficient Implementation of Weighted ENO Schemes. *J. Comp. Phys.*, 126(130):202–228, 1996.

[15] M. Käser. *Adaptive Methods for the Numerical Simulation of Transport Processes.* PhD thesis, Institute of Numerical Mathematics and Scientific Computing, University of Munich, Germany, 2003.

[16] M. Käser. and A. Iske. ADER Schemes for the Solution of Conservation Laws on Adaptive Triangulations. Mathematical Methods and Modelling in Hydrocarbon Exploration and Production. Mathematics in Industry , Vol. 7:323–385. Springer-Verlag, 2005.

[17] M. Käser and A. Iske. Adaptive ADER Schemes for the Solution of Scalar Non-Linear Hyperbolic Problems. *J. Comput. Phys.*, 205:486–508, 2005.

[18] Kolgan V. P. Application of the Principle of Minimum Derivatives to the Construction of Difference Schemes for Computing Discontinuous Solutions of Gas dynamics (in Russian). *Uch. Zap. TsaGI, Russia*, 3(6):68–77, 1972.

[19] H. Schardin. In Proc. VII Int. Cong. High Speed Photg. Darmstadt. O. Helwich Verlag, 1965.

[20] T. Schwartzkopff. *Finite–Volumen Verfahren hoher Ordnung und heterogene Gebietszerlegung ü die numerische Aeroakustik*. PhD thesis, Institut für Aero- un Gasdynamik, Universität Stuttgart, Germany, 2005.

[21] T. Schwartzkopff, Munz C.D, and E. F. Toro. ADER: High-Order Approach for Linear Hyperbolic Systems in 2D. *J. Scientific Computing*, 17:231–240, 2002.

[22] T. Schwartzkopff, M. Dumbser, and Munz C.D. Fast High-Order ADER Schemes or Linear Hyperbolic Equations. *J. Comput. Phys.*, 197:532–539, 2004.

[23] C. Shu and S. Osher. Efficient Implementation of Essentially Non–oscillatory Shock–Capturing Schemes II. *J. Comput. Phys.*, 83:32–78, 1988.

[24] C. W. Shu and S. Osher. Efficient Implementation of Essentially Non–oscillatory Shock–Capturing Schemes. *J. Comput. Phys.*, 77:439–471, 1988.

[25] Y. Takakura and E. F. Toro. Arbitrarily Accurate Non-Oscillatory Schemes for a Non-Linear Conservation Law. *J. Computational Fluid Dynamics*, 11(1):7–18, 2002.

[26] V. A. Titarev and E. F. Toro. ADER: Arbitrary High Order Godunov Approach. *J. Scientific Computing*, 17:609–618, 2002.

[27] V. A. Titarev and E. F. Toro. ADER Schemes for Three-Dimensional Hyperbolic Systems. *J. Comput. Phys.*, 204:715–736, 2005.

[28] E. F. Toro. Primitive, Conservative and Adaptive Schemes for Hyperbolic Conservation Laws. In *Numerical Methods for Wave Propagation. Toro, E. F. and Clarke, J. F. (Editors)*, pages 323–385. Kluwer Academic Publishers, 1998.

[29] E. F. Toro, R. C. Millington, and L. A. M. Nejad. Towards Very High–Order Godunov Schemes. In *Godunov Methods: Theory and Applications. Edited Review, E. F. Toro (Editor)*, pages 905–937. Kluwer Academic/Plenum Publishers, 2001.

[30] E. F. Toro and V. A. Titarev. Solution of the Generalised Riemann Problem for Advection-Reaction Equations. *Proc. Roy. Soc. London A*, 458:271–281, 2002.

[31] E. F. Toro and V. A. Titarev. ADER Schemes for Scalar Hyperbolic Conservation Laws with Source Terms in Three Space Dimensions. *J. Comput. Phys.*, 202(1):196–215, 2005.

[32] E. F Toro and Titarev V. A. Derivative Riemann Solvers for Systems of Conservation Laws and ADER Methods. *J. Comput Phys.*, 212(1):150–165, 2006.

[33] E. F Toro and A. Hidalgo. ADER finite volume schemes for non-linear reaction diffusion equations. *Appl. Numer. Math.*, (submitted), 2007. Also published as: Isaac Newton Institute for Mathematical Sciences, Cambridge University, UK, Preprint Series NI07011-NPA, 2007.

[34] B. van Leer. Towards the Ultimate Conservative Difference Scheme I. The Quest for Monotonicity. *Lecture Notes in Physics*, 18:163–168, 1973.

[35] B. van Leer. On the Relationship between the Upwind-Differencing Schemes of Godunov, Engquist-Osher and Roe. *SIAM J. Sci. Stat. Comput.* 5(1):1-20, 1985.

[36] G. Vignoli, V. A. Titarev and E. F. Toro. ADER schemes for the shallow water equations in channel with irregular bottom elevation. *J. Comput. Phys.* (submitted), 2007.